ELSEVIER

Journal of Photochemistry and Photobiology A: Chemistry 152 (2002) 199–205

Journal of Photochemistry and Photobiology A:Chemistry

www.elsevier.com/locate/jphotochem

Electronic energy transfer efficiency of mixed solutions of the donor–acceptor pairs: coumarin derivatives—acridine orange

K.A. Kozyra [a,*], J.R. Heldt [a], H.A. Diehl [c], J. Heldt [a,b]

[a] *Institute of Experimental Physics, University of Gdańsk, ul. Wita Stwosza 57, 80-952 Gdańsk, Poland*
[b] *Institute of Physics, Pomeranian Pedagogical Academy, ul. Arciszewskiego 23A, 76-200 Słupsk, Poland*
[c] *Biophysics Group, Fachbereich 1 (Physics), University Bremen, D-28334 Bremen, Germany*

Received 30 May 2001; received in revised form 21 May 2002; accepted 28 May 2002

Abstract

Excitation energy transfer between coumarin derivatives and acridine orange (AO) in solutions of two different viscosities has been studied. The rate constants of the electronic energy transfer (k_{ET}) and critical radius (R_0) were determined for coumarin derivatives as donors and AO as acceptor. The obtained values of k_{ET} and R_0 indicate that dipole–dipole interaction between D–A pairs is responsible for the energy transfer mechanism. The experimental data of energy transfer efficiency are well described by the Förster theory.

Keywords: Coumarins; Excitation energy transfer; R_0 and k_{ET} determination

1. Introduction

The coumarins establish a family of dyes which are applicable in different fields of science and technology. In quantum and non-linear optics the coumarin derivatives are used as an active medium in dye lasers [1–4] and as a doping dye of polymers used as electro-optical materials for light modulators and frequency doubling devices [5]. In chemistry some coumarin derivatives are used as fluorescence derivatization reagents for liquid chromatography [6], fluorescence probes for protein studies [7] and as fluorescent ionophores [8]. In medicine coumarin derivatives are used as anticoagulants [9], as fluorescent indicators for the physiological pH region [10,11] and as fluorescent probes to determine the rigidity and fluidity of living cells and its surrounding medium [3,12,13]. Coumarin derivatives have intensively been used as model substrates to quantify the enzymatic activity of microsomal monooxygenases [32,33].

Coumarin derivatives often constitute one or both chromophores in a bichromophoric molecule [14]. Such molecules have been a subject of considerable interest in numerous fields, i.e., photophysical processes of biological systems [15,16], polymers [17], pharmacology [18] and dye laser physics [1,5]. For these molecules the effectivity of the intramolecular energy transfer mechanism (the long-range dipole–dipole interaction) favours its many applications. The same mechanism is responsible for intermolecular electronic energy transfer between donor–acceptor pairs of many molecules.

In this paper, we report results of intermolecular electronic energy transfer studies between four coumarin derivatives (donors) and acridine orange (acceptor) pairs in methanol and glycerol. The studies in viscous glycerol were performed with selected pairs only. The coumarin derivatives used in the study differ from each other by the kind of the alkoxy group substituting the hydrogen atom at position 7 of the parent coumarin molecule. From the viewpoint of future biophysical applications, it seems interesting to study the radiationless electronic energy transfer for this set of molecules in particularly to determine the influence of the 7-alkoxy functional groups on the energy transfer mechanism, i.e., on the parameters describing this phenomenon.

2. Experimental details

In the present paper, we study 7-alkoxycoumarins with following substituents at the 7 position of the parent molecule (see Fig. 1.): $R_1 = –OCH_3$ (7-methoxycoumarin, 7MOC), $–OC_2H_5$ (7-ethoxycoumarin, 7EOC), $–OC_8H_{17}$ (7-octyloxycoumarin, 7OcOC), $–OC_{10}H_{21}$ (7-decyloxycoumarin, 7DeOC). Synthesis and purification of these

* Corresponding author.
E-mail address: dokkat@julia.univ.gda.pl (K.A. Kozyra).

1010-6030/02/$ – see front matter
PII: S1010-6030(02)00230-7

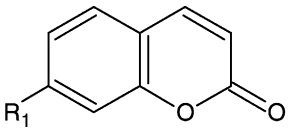

$R_1 = OCH_3$ – **7MOC**
$R_1 = OC_2H_5$ – **7EOC**
$R_1 = OC_8H_{17}$ – **7OcOC**
$R_1 = OC_{10}H_{21}$ – **7DecOC**

Fig. 1. Structure formula of the coumarin derivatives used.

coumarin derivatives have been described [12]. The 3,6-bis(dimethylamino)acridine (acridine orange—AO) was purchased from Merck and used without further purification. The solvents methanol and glycerol were of spectroscopic grade.

The absorption spectra of the dyes were measured on a Shimadzu UV-2401PC spectrophotometer. The fluorescence spectra of the compounds and their mixtures were performed with a Shimadzu RF-5301 spectrofluoro photometer. Measurements were carried out using the triangular cuvette with frontal excitation to minimize the effect of reabsorption of donor emission by the acceptor. The emission was observed perpendicular to the direction of the exciting beam. Thus the errors due to fluorescence reabsorption were reduced in a way that mathematical corrections were superfluous.

The quantum yield was determined by comparison with a standard solution. Quinine sulphate in 0.5 N sulphuric acid was used as a reference compound, which quantum yield is $\Phi_F = 0.55 \pm 0.03$ [19]. The fluorescence quantum yield was calculated according to the relationship [20]:

$$\Phi_F = \Phi_F^S \frac{\int_0^\infty I_F(\tilde{\nu})\,d\tilde{\nu}}{\int_0^\infty I_F^S(\tilde{\nu})\,d\tilde{\nu}} \frac{1-10^{-A_S}}{1-10^{-A}} \frac{n^2}{n_S^2}, \quad (1)$$

where Φ_F^S is the quantum yield of the standard solution, the integrals $\int_0^\infty I_F(\tilde{\nu})\,d\tilde{\nu}$ and $\int_0^\infty I_F^S(\tilde{\nu})\,d\tilde{\nu}$ are the areas under the emission curves of the investigated and standard compound, respectively, A and A_S are the respective absorbances of the solutions at the wavelength of excitation, n and n_S is the refractive index of the studied and standard samples, respectively.

The fluorescence decay time τ_F^D of coumarin derivatives in solution was calculated using the formula:

$$\tau_F^D = \frac{\Phi_F}{k_F}, \quad (2)$$

where k_F is the fluorescence rate constant. As it was shown earlier [24] the absorption and fluorescence spectra of the coumarins under study fulfil the mirror symmetry relation. For these compounds the theoretical absorption rate coefficient k_A, expressed according to Strickler and Berg [21] by the absorption and emission integrals equals:

$$k_A = \frac{8000\pi \ln 10 c n_F^3}{N n_A} \langle \tilde{\nu}_F^{-3} \rangle^{-1} \frac{g_e}{g_g} \int_0^\infty \frac{\varepsilon(\tilde{\nu})\,d\tilde{\nu}}{\tilde{\nu}}, \quad (3)$$

where

$$\langle \tilde{\nu}_F^{-3} \rangle^{-1} = \int_0^\infty I_F(\tilde{\nu})\,d\tilde{\nu} \left(\int_0^\infty \frac{I_F(\tilde{\nu})}{\tilde{\nu}^3}\,d\tilde{\nu} \right)^{-1}, \quad (4)$$

n_F, n_A are the solvent refraction indices for the wavelengths corresponding to the fluorescence and the absorption band, respectively, N is the Avogadro's number, c denotes the velocity of light in vacuum, $\varepsilon(\tilde{\nu})$ is the molar absorption coefficient, $I_F(\tilde{\nu})$ describes the normalized energy distribution of the fluorescence spectrum, and g_e, g_g are degeneracy coefficients equal to one for the excited and the ground singlet state, respectively [21,22].

It was shown by many authors [19,21,22] that for those molecules the fluorescence rate constant k_F equals to the absorption rate coefficient k_A, i.e., $k_F = k_A$. Making use of this equality the fluorescence decay time, τ_F^D, of the donor molecules has been determined using Eqs. (2) and (3).

Table 1 assembles the determined Φ_F and τ_F^D data of the compounds under study. The instrumental error of Φ_F determination is within 10% whereas the τ_F^D calculated data agree with the experimental values in the range of instrumental error limit equal to 5% [24]. Since the estimated lifetimes, τ_F^D, are very short as can be seen in Table 1, it is less probable that during the lifetime of excited state depopulating collision occurs in both solutions.

Table 1
Fluorescence quantum yields, Φ_D^0, fluorescence decay times, τ_F^D, radiative transition probabilities, k_F, and spectral overlap integral, $J_{DA}(\tilde{\nu})$, of coumarin derivatives in methanol and glycerol at room temperature

Donor	Solvent	$\Phi_D^{0\,a}$	k_F ($\times 10^{-7}$ s^{-1})[b]	τ_F^D (ns)[c]	$J_{DA}(\tilde{\nu})$ ($\times 10^{-14}$ l cm^3 mol^{-1})[d]
7MOC	M	0.033	13.16	0.25	1.20497
	G	0.430	18.52	2.32	0.88672
7EOC	M	0.050	12.24	0.40	1.27213
	G	0.570	25.45	2.23	0.80485
7OcOC	M	0.062	10.90	0.56	1.27865
7DecOC	M	0.064	12.22	0.52	1.28446

[a] Quantum yield of the pure donor Eq. (1).
[b] Fluorescence rate constant calculated by Eq. (3).
[c] Fluorescence lifetime of the pure donor determined according to Eq. (2).
[d] The spectral overlap integral calculated using Eq. (5).

3. Results and discussion

3.1. One-compound solution

As an example the absorption and emission spectra of the donor molecule (7EOC) and acceptor molecule (AO) in methanol are shown in Fig. 2a, whereas Fig. 2b shows the donor emission and the acceptor absorption spectra and the calculated overlap integral of the 7EOC–AO pair. The overlap of the A-Ab and D-Em spectra suggests (see Fig. 2) that the donor–acceptor energy transfer can take place. The spectral overlap integral was calculated using the formula [23]:

$$J_{DA}(\tilde{\nu}) = \int_0^{\infty} \frac{I_{FD}(\tilde{\nu})\varepsilon_A(\tilde{\nu})}{\tilde{\nu}^4}\, d\tilde{\nu}, \quad (5)$$

where $I_{FD}(\tilde{\nu})$ is the spectral distribution of the donor fluorescence intensity normalized to unity and $\varepsilon_A(\tilde{\nu})$ the molar extinction coefficient of the acceptor.

The values of the spectral overlap integral for all donor–acceptor systems under study are listed in Table 1. The values of the various donor–acceptor pairs in methanol and some pairs in glycerol do not show significant differences. The $J_{DA}(\tilde{\nu})$ values increases with increasing chain

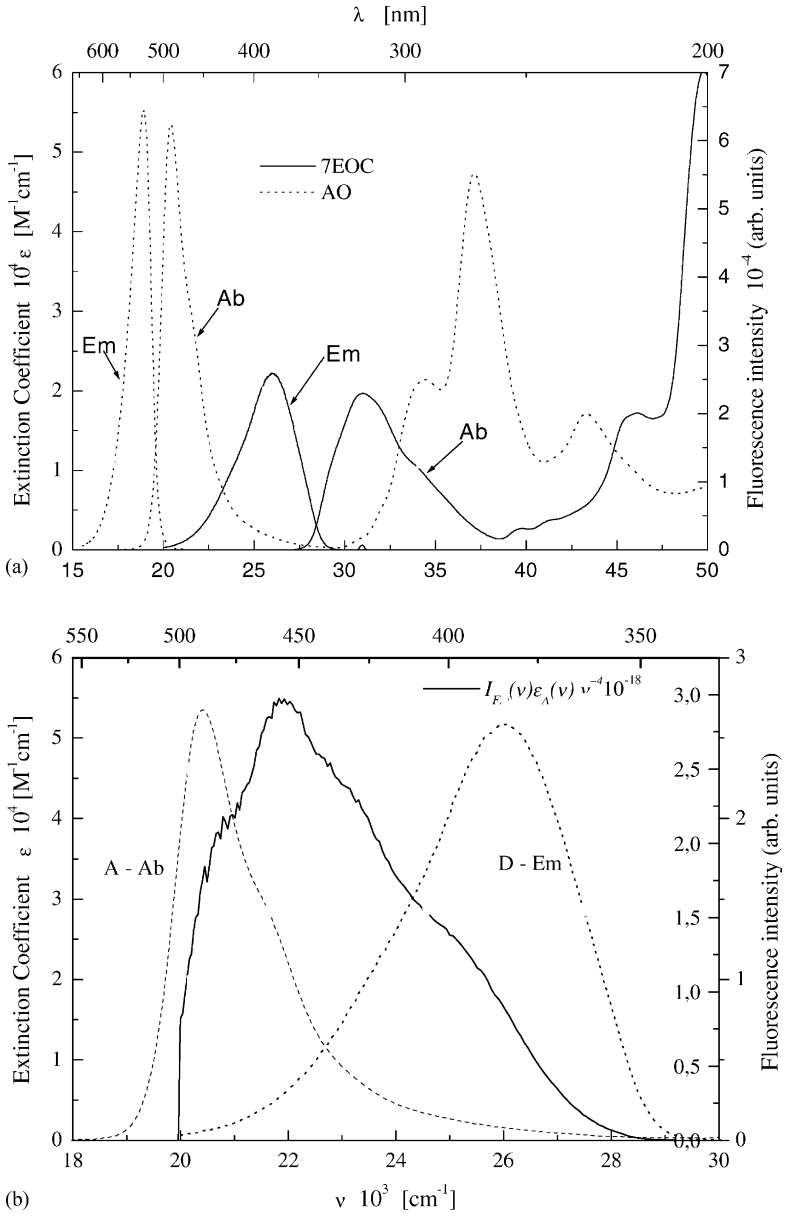

Fig. 2. (a) Normalized fluorescence and absorption spectra of the compounds 7EOC and AO. (b) The overlap spectrum between donor emission 7EOC and acceptor absorption AO.

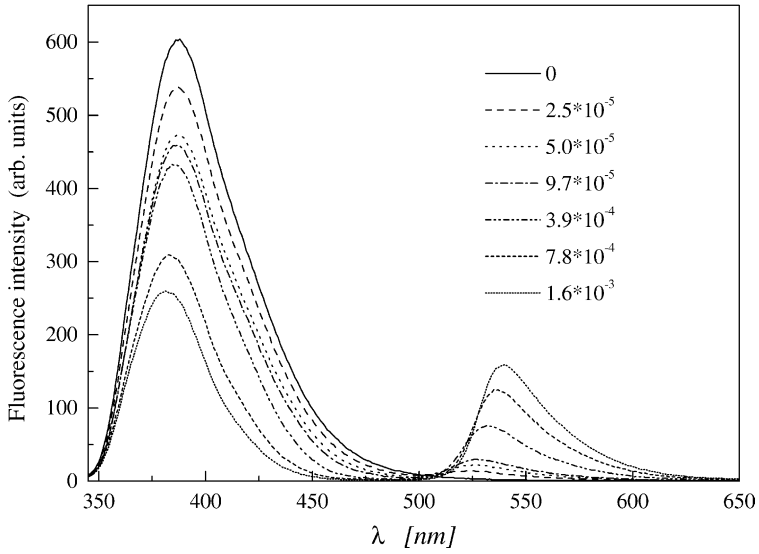

Fig. 3. Emission spectra of 7MOC and AO in glycerol in the presence of various concentration of AO. Donor concentration $C_D = 1.125 \times 10^{-4}$ M.

length of the alkoxy functional groups substituted at position 7 of the donor molecule. It must be noted that the substituent at position 7 of coumarin, shifts the fluorescence spectra to longer wavelengths, increases the quantum yield and the mean fluorescence lifetime. The observed changes of the data can be explained by the electronic transition moment changes in the molecule, caused by the weak donation potential of the substituent [24].

3.2. The fluorescence quenching phenomena

Fig. 3 shows the fluorescence spectra of the donor (7MOC) obtained in the presence of the acceptor (AO) molecule at its various concentrations. The spectra have been obtained at the donor constant concentration ($C_D = 1.125 \times 10^{-4}$ M). The acceptor concentration changes from 1.2×10^{-5} to 1.5×10^{-3} M. The solutions were excited at $\lambda_{exc} = 340$ nm. From these spectra it is obvious that increasing the acceptor concentration a successive decrease occurs in the donor fluorescence intensity. The same dependence is noted for all other donor–acceptor pairs under study. It should be noted that we did not detect any extra absorption band in the spectral range 200–600 nm for the mixture of the coumarin derivatives and AO. It points to the absence of any detectable ground-state complexes of the donor acceptor pairs in the solution.

Analysing the emission spectra of all donor–acceptor pairs a blue shift of the donor fluorescence spectrum is observed with increasing acceptor concentration. The observed shift is about 5 nm by concentration changes of AO from 2.5×10^{-5} to 1.6×10^{-3} M. This finding can be attributable to the radiative transfer phenomena [25]. It is known that the acceptor molecules quench the longer wavelength portion of donor fluorescence spectrum more effectively than the shorter one. Whereas the simultaneous successive red shift of the acceptor fluorescence maximum can be attributed to reabsorption and radiative migration [25,26]. It results because by the absorption depth of the exciting light (about 2 mm) the reabsorption is not completely reduced. The changes in the λ_{max} of the acceptor fluorescence were observed also in absence of the donor (data not shown). This red shift of AO spectra is independent on coumarin derivatives, thus this phenomena is not important for the fluorescence quenching studies therefore will not be discussed here. In Fig. 3, the noted spectra changes distinctly show that the fluorescence of coumarin derivatives was effectively quenched by AO molecules.

The quenching process, as it follows from the fluorescence quantum yield ratio of the donor versus the acceptor concentration [C_A] (see Fig. 4), is described by the Stern–Volmer relation [27]:

$$\frac{\Phi_D^0}{\Phi_D} = 1 + K_{SV}[C_A] = 1 + k_{ET}\tau_F^D[C_A], \quad (6)$$

where Φ_D^0 and Φ_D are the quantum yield of the donor without and with acceptor molecules in the solution, K_{SV} is the Stern–Volmer constant, k_{ET} the energy transfer rate constant and τ_F^D the fluorescence decay time of donor molecules under study.

Fig. 4 shows the Stern–Volmer plots of the fluorescence quenching of selected coumarin derivatives in methanol and glycerol using AO as a quencher. Experimental data follow the Stern–Volmer dependence well in the concentration range of the quencher used. Determining the slopes from this drawing, i.e., the K_{SV} values, the quenching rate constants k_{ET} can be determined. The k_{ET} data obtained are listed in Table 2. The values of k_{ET} comprise 10^{11}–10^{12} l mol^{-1} s^{-1} which is substantially higher than that noted for the bimolecular rate constants controlled by diffusion. Diffusion rate

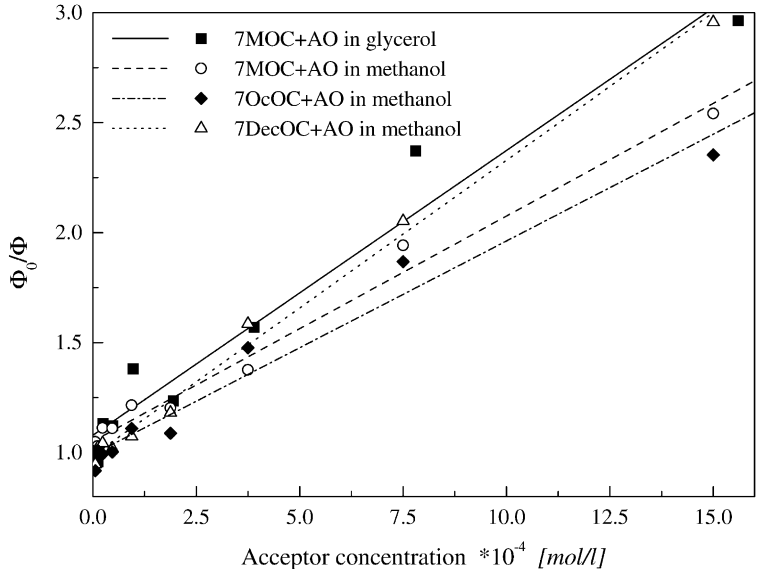

Fig. 4. Stern–Volmer plots of the fluorescence quenching of coumarin derivatives in methanol and glycerol solutions using AO as a quencher.

constants calculated according to the Debye equation [28] for methanol and glycerol at room temperature are $k_{DIFF} = 9.7 \times 10^9$ and $k_{DIFF} = 4 \times 10^6\,l\,mol^{-1}\,s^{-1}$, respectively. The big difference noted between the k_{ET} and k_{DIFF} values indicate a diffusion-free mechanism for the electron energy transfer of the studied D–A pairs. On this base we can state that the dipole–dipole mechanism is responsible for the radiationless energy transfer of the D–A pairs under study. The values of k_{ET} for 7MOC–AO and 7EOC–AO pairs in methanol and glycerol are different, the k_{ET} value in methanol solution is about five times greater than in glycerol. This difference does not exceed 1 order of magnitude, is smaller than that given earlier for k_{DIFF} and k_{ET}. Taking this into consideration we believe that the dipole–dipole mechanism is confirmed and is the dominating quenching mechanism of the donor fluorescence in the D–A solutions.

If the energy transfer between the donor and acceptor molecules is caused by a dipole–dipole long-range interaction in accordance to Förster's theory [29], the energy transfer rate constant k_{ET} is expressed by [25,29]:

$$k_{ET} = \frac{9000 \ln 10 \kappa^2 \Phi_D^0}{128\pi^5 N r^6 \tau_F^D} \int_0^\infty \frac{I_{DF}(\tilde{\nu})\varepsilon_A(\tilde{\nu})}{\tilde{\nu}^4}\,d\tilde{\nu}, \quad (7)$$

where r is the distance between D and A molecules (in cm), κ the orientation factor which takes into account the angles between the transition moments of the D and A molecules, the other denotation have the same meaning as in Eq. (5). The viscosities of glycerol and methanol solvents are very different ($\eta_{glycerol} = 1.49$ and $\eta_{methanol} = 0.6 \times 10^{-3}$ Pa s), therefore in accordance with [19,30] we assume for the investigated systems in glycerol $\langle\kappa^2\rangle = 0.472$ and in methanol $\langle\kappa^2\rangle = 2/3$. Taking the experimental values of the spectral

Table 2
Experimentally determined critical transfer distance, R_0, and rate constants for energy transfer, k_{ET}, of various coumarin derivatives

Donor	Solvent	K_{SV} ($l\,mol^{-1}$)[a]	k_{ET} ($\times 10^{12}\,l\,mol^{-1}\,s^{-1}$)[b]	R_0 (Å)[c]	R_0 (Å)[d]	$[C]_{1/2}$ ($\times 10^4\,mol\,l^{-1}$)[e]	R_0 (Å)[f]	R_S (Å)[g]
7MOC	M	1024	4.09	65.0	74.1	9.15	75.7	4.8
	G	1268	0.54	88.3	79.5	6.0	87.1	4.8
7EOC	M	1115	2.78	70.0	76.2	8.5	77.6	4.9
	G	1282	0.57	91.0	81.5	5.6	89.2	4.9
7OcOC	M	958	1.71	72.8	72.4	5.0	74.7	6.2
7DecOC	M	1343	2.58	73.2	81.1	7.0	82.7	6.7

[a] Experimentally determined from Stern–Volmer plots.
[b] Calculated using the Eq. (6).
[c] Theoretically calculated using the Eq. (8).
[d] Theoretically calculated using the Eq. (9).
[e] Determined from the Förster quenching theory.
[f] Theoretically calculated using the Eq. (13).
[g] The radius of donor and acceptor collision complex for collision transfer where R_S is sum of donor and acceptor radii.

overlap integral $J_{DA}(\tilde{\nu})$ (see Table 1), the Förster distance R_0 at which the transfer rate constant k_{ET} is equal to the fluorescence decay rate constant of the donor in the absence of acceptor, has been calculated using the formula:

$$R_0^6 = \frac{9000 \ln 10 \kappa^2 \Phi_D^0}{128\pi^5 n^4 N} \int_0^\infty \frac{I_{DF}(\tilde{\nu})\varepsilon_A(\tilde{\nu})}{\tilde{\nu}^4} d\tilde{\nu}. \quad (8)$$

The R_0 data obtained from Eq. (7) are assembled in Table 2. The k_{ET} and R_0 values have been calculated assuming that the distance between all the donor and acceptor pairs is constant, e.g. as for solid state or bichromophoric systems. For its solution Eq. (7) must be modified [31] to

$$k'_{ET} = \frac{R_0^3}{(7.35 \times 10^{-8})^3 \tau_F^D}. \quad (9)$$

The R_0 data, calculated using Eq. (9) and the k'_{ET} values obtained from the Stern–Volmer dependence are inserted in Table 2, too. As can be seen analysing the data of Table 2 the experimental values of R_0 obtained from the Stern–Volmer plots are in good conformity with those calculated using formula (8), and both indicate that the energy transfer occurs on the distance larger than the sum of the collision radii, $R_D + R_A$. The sum of collision radii of coumarin and AO is about 4.5–7 Å. The values of R_0 are larger for 7DecOC, possessing a long alkoxy chain, than for the other coumarin derivatives (7MOC, 7EOC, 7OcOC). This dependence is a result of its higher fluorescence quantum yield and longer fluorescence decay time. The values of R_0 for 7MOC and 7EOC in glycerol are larger than those determined for methanol solutions. This difference (about 30%) is a result of the fluorescence quantum yield differences noted for glycerol and methanol donor—7MOC and 7EOC solutions.

3.3. Donor fluorescence quantum yield in excitation energy transfer

Transfer of excitation energy from donor to acceptor causes a decrease of the quantum yield of the donor molecule. The quantum yield of the donor determined in the presence, Φ_D^0, and in the absence of the acceptor, Φ_D, permits to calculate the energy transfer efficiency, Φ_T, in an independent way. According to the Förster theory [25] the energy transfer efficiency Φ_T as well as the ratio, Φ_D/Φ_D^0, for fluorescence quantum yields depend from the reduced concentration γ_{DA} for donor-overlapping as follows:

$$\frac{\Phi_D}{\Phi_D^0} = 1 - \Phi_T = 1 - \sqrt{\pi}\gamma_{DA} \exp(\gamma_{DA})^2 [1 - \mathrm{erf}(\gamma_{DA})], \quad (10)$$

where $\mathrm{erf}(\gamma_{DA})$ is the Gaussian error function described by

$$\mathrm{erf}(x) = 2\sqrt{\pi} \int_0^x \exp(-x^2)\, dx \quad (11)$$

$\gamma_{DA} = C_A/C_{0A}$ is the reduced concentration for donor-overlapping [26,29], where C_A is the acceptor concentration and C_{0A} is a critical concentration. C_{0A} is related to the critical transfer distance R_0 as follows [26]:

$$C_{0A} = \frac{3000}{4\pi N R_0^3}. \quad (12)$$

Fig. 5 shows relative fluorescence quantum yield data of the systems under study versus $\log[C_A]$ and the theoretical curves calculated from Eq. (10). The Förster curves were calculated for the R_0 values obtained from Eq. (8). The best fit of the experimental points with the curve obtained from the Förster theory are shown in Fig. 5. It can be seen that the

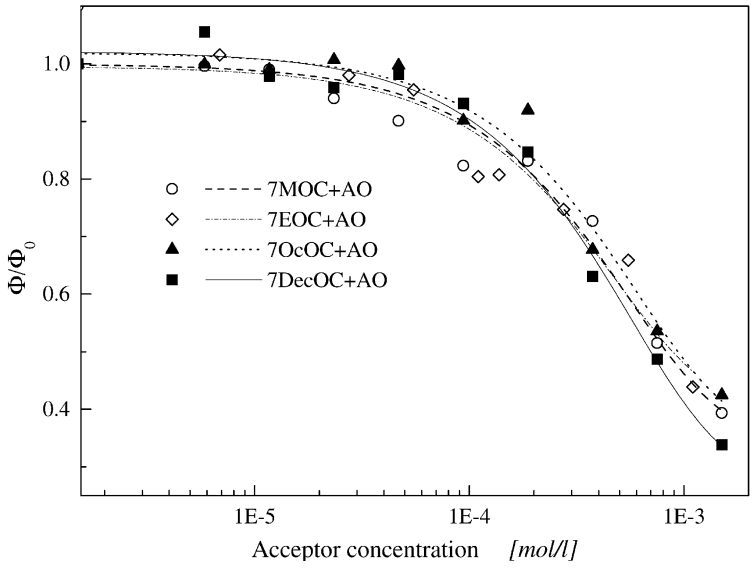

Fig. 5. Relative donor fluorescence quantum yield Φ/Φ_0 in presence of acceptor molecules dissolved in methanol. The full and dashed curves are calculated from Eq. (10). The points represent the experimental results.

empirical results are in good agreement with the predictions of the Förster theory.

This conformity allows us to calculate the critical radius of energy transfer R_0 by means of following formula [31]:

$$R_0 = 7.35([C_{1/2}])^{-1/3}, \quad (13)$$

where $[C_{1/2}]$ is the acceptor concentration at which the fluorescence intensity of the donor is reduced to half. The $[C_{1/2}]$ values of the acceptor concentration for all D–A pairs under study are summarized in Table 2. The R_0 values calculated from Eq. (13) are listed in Table 2. Analysing all R_0 values obtained from Eqs. (8), (9) and (13), it indicates that the critical distance value R_0 obtained from the spectral overlap integral (Eq. (8)) and from the main Eqs. (9) and (13) are equal in the error range of its determination. The differences are less than 9%. Also, it follows that the R_0 values show a weak dependence on the volume of donor molecule, i.e., coumarin derivatives. It must be noted that R_0 values are smaller for methanol solutions. The difference is about 5% in comparison to the R_0 values obtained for glycerol solutions. The performed studies show that the R_0 values of 7-alkoxycoumarin–AO D–A pairs show a regular dependence from the 7-alkoxy substituent of coumarin with an exception for 7OcOC–AO pair for R_0 values determined using Eqs. (9) and (13). Big differences between the values of the collision radii ($R_{coll} \sim 5$–7 Å) and the critical radius of energy transfer ($R_0 \sim 65$–90 Å) are noticed. This points that for 7-alkoxycoumarin—AO (D–A) pairs a dipole–dipole interaction is responsible for the energy transfer mechanism. Also that energy transfer rate constant k_{ET} depends on the solvent and used donor molecule (see Table 1). The k_{ET} value decreases with increasing of 7-alkoxy substituent.

Acknowledgements

This work is in part supported by KBN grant 127/E-335/S/2000 funding scientific co-operation between the University of Gdansk and the University of Bremen, and grant BW 5200-5-0206-01 of the University of Gdansk.

References

[1] K.H. Drexhage, in: F.P. Schafer (Ed.), Dye Lasers, Springer, New York, 1977.
[2] V. Masilamani, B.M. Sivaram, J. Lumin. 27 (1982) 137.
[3] M.S.A. Abdel-Mottaleb, M.S. Antonious, M.M. Abo-Aly, L.F.M. Ismaiel, B.A. El-Sayed, A.M.K. Sherief, J. Photochem. Photobiol. A 50 (1989) 259.
[4] A.N. Fletcher, M.E. Pietrak, D.E. Bliss, Appl. Phys. B 42 (1987) 79.
[5] K.D. Singer, S.L. Lalamo, J.E. Sohn, R.D. Small, in: D.S. Chemla, J. Zyss (Eds.), Nonlinear Optical Properties of Organic Molecules and Crystals, Academic Press, Orlando, 1987 (Chapter II-8).; J.F. Nicoud, R.J. Twieg, in: D.S. Chemla, J. Zyss (Eds.), Nonlinear Optical Properties of Organic Molecules and Crystals, Academic Press, Orlando, 1987 (Chapter II-3).
[6] Ch.R. Moyaln, J. Phys. Chem. 98 (1994) 13513.
[7] G.E. Dobrestov, Fluorescent Probes for Study Cells, Membranes and Proteins, Nauka, Moscow, 1989.
[8] A. Takadate, T. Masuda, C. Murata, T. Tanaka, M. Irikura, S. Goya, Anal. Sci. 8 (1992) 695.
[9] A. Takadate, T. Masuda, C. Murata, T. Tanaka, M. Irikura, S. Goya, Anal. Sci. 11 (1995) 97.
[10] O.S. Wolfbeis, Z.F. Phys. Chem. N.F. 125 (1981) 15.
[11] O.S. Wolfbeis, E. Furlinger, H. Kroneis, H.Z. Marsoner, Anal. Chem. 314 (1983) 577.
[12] R. Düren, H. Diehl, J. Chromatogr. 445 (1988) 49.
[13] M. Engelke, Th. Behmann, F. Ojeda, H.A. Diehl, Chem. Phys. Lipids 72 (1994) 35.
[14] J. Mugnier, J. Pouget, J. Bourson, B. Baleur, J. Lumin. 33 (1985) 273.
[15] L. Stryer, Am. Rev. Biochem. 47 (1978) 819; and reference cited therein.
[16] E. Katchalski-Katzir, E. Haas, I.Z. Steinberg, Ann. N.Y. Acad. Sci. 366 (1981) 44.
[17] G.H. Frederickson, H.C. Andersen, C.W. Frank, J. Chem. Phys. 79 (1983) 3572; G.H. Frederickson, H.C. Andersen, C.W. Frank, Macromolecules 17 (1984) 54; and reference cited therein.
[18] C. Thiery, Mol. Photochem. 2 (1970) 1.
[19] C.A. Parker, Photoluminescence of Solutions with Applications to Photochemistry and Analytical Chemistry, Elsevier, Amsterdam, 1968.
[20] A. Kawski, G. Liszczek, B. Kukliński, N. Nowosielski, Z. Naturforsh. A 49 (1994) 824.
[21] S.J. Strickler, R.A. Berg, J. Chem. Phys. 37 (1962) 814.
[22] J.B. Birks, D.J. Dyson, Proc. R. Soc. London A 275 (1963) 135.
[23] J.R. Lakowicz, Principles of Fluorescence Spectroscopy, Plenum Press, New York, 1983 (Chapter 10).
[24] J.R. Heldt, J. Heldt, M. Stoñ, H.A. Diehl, Spectrochimica Acta Part A 51 (1995) 1549.
[25] J.B. Birks, Photophysics of Aromatic Molecules, Wiley Interscience, New York, 1970.
[26] K.K. Pandey, T.C. Pant, J. Lumin. 47 (1991) 319.
[27] O. Stern, M. Volmer, Phys. Z. 20 (1919) 183.
[28] C. Lin, A. Dienes, J. Appl. Phys. 44 (1973) 5050.
[29] Th. Förster, Fluoreszenz Organischer Verbindungen, Vanderhoeck und Ruprecht, Götingen, 1951.
[30] A. Kawski, E. Kuteñ, J. Kamiński, J. Phys. B 6 (1973) 1907.
[31] N.J. Turro, Modern Molecular Photochemistry, Benjamin/Cummings, California, 1987.
[32] U. Schröder, H. Diehl, Eur. Biophys. J. 14 (1987) 329.
[33] V. Ullrich, P. Weber, H.-S. Z. Physiol. Chem. 353 (1972) 1171.